

Athlete rating in multi-competitor games with scored outcomes via monotone transformations

Jonathan Che and Mark Glickman

Harvard University

Abstract:

Sports organizations often want to estimate athlete strengths. For games with scored outcomes, a common approach is to assume observed game scores follow a normal distribution conditional on athletes' latent abilities, which may change over time. In many games, however, this assumption of conditional normality does not hold. To estimate athletes' time-varying latent abilities using non-normal game score data, we propose a Bayesian dynamic linear model with flexible monotone response transformations. Our model learns nonlinear monotone transformations to address non-normality in athlete scores and can be easily fit using standard regression and optimization routines. We demonstrate our method on data from several Olympic sports, including biathlon, diving, rugby, and fencing.

Keywords and phrases: Dynamic linear model, Kalman filter.

1. Introduction

Sports and gaming organizations, athletes, and fans often wish to estimate how good athletes are at their sports. This problem of athlete rating can affect planning and preparation for games, at both organizational and individual levels. For example, ratings may influence how sports organizations allocate resources across their athletes prior to an event to maximize their chances of winning. Ratings may also be used for designing tournaments and league play. This includes pairing athletes with similar estimated abilities in head-to-head competitions, dividing a large set of competitors into smaller tournaments according to skill level, or selecting top athletes to compete in elite “by invitation only” events.

Approaches that rely on statistical modeling enable researchers to infer athletes' abilities from their game outcomes in a principled manner. A typical method for constructing athlete ratings treats each athlete's strength as a latent parameter (or vector of parameters) within a probability model. The models then use observed game outcomes to estimate the latent ability parameters, which may be thought of as fixed or varying over time.

A variety of methods for estimating dynamic (i.e., time-varying) athlete ratings have been proposed for games with binary (i.e., win/loss) outcomes, or with rank-ordered outcomes. For multi-competitor games, approaches to rating competitors typically extend the Plackett-Luce model (Plackett, 1975) through

the evolution of the latent ability parameters. For example, [Glickman and Hennessey \(2015\)](#) models the evolution as a discrete stochastic process, [Caron and Teh \(2012\)](#) uses a nonparametric stochastic process, [Baker and McHale \(2015a\)](#) interpolates abilities between discrete time points, and [McKeough \(2020\)](#) considers parametric growth curves over time. Dynamic models have also been proposed for head-to-head games with win/loss outcomes, in both team ([Herbrich, Minka and Graepel, 2006](#)) and individual ([Glickman, 1999, 2001](#); [Cattelan, Varin and Firth, 2013](#); [Baker and McHale, 2015b](#)) game settings.

Score outcomes are more granular than rank-order outcomes; as a result, models that effectively use score data may outperform models that only use ranking data. Observed rank outcomes can be viewed as partially censored score outcomes. For example, in a race, each runner’s performance can be recorded as a race time, which can then be mapped into a race placement. In this instance, the race placement is the ranking and the race time is the score. Score data can potentially provide information, particularly about the gaps in performances between athletes, which may be useful to a rating model.

While various dynamic models that use score or score-related information have been proposed for head-to-head games ([Harville, 1977](#); [Glickman and Stern, 1998](#); [Lopez, Matthews and Baumer, 2018](#); [Ingram, 2019](#); [Kovalchik, 2020](#)), we are unaware of similar work for multi-competitor games. In this paper, we extend the normal dynamic linear model (DLM) proposed by [Harville \(1977\)](#) and [Glickman and Stern \(1998\)](#) to rate athletes who compete in multi-competitor games. DLMS provide a simple, natural framework for rating athletes in multi-competitor games with scored outcomes. They assume that an athlete’s latent ability varies across time periods as a discrete stochastic process, and that an athlete’s scores are normally distributed around their latent ability parameter within each time period.

Athletes’ game scores, however, can often be heavy-tailed or skewed, which suggests that the normal assumption in DLMS may not hold. Furthermore, games with blowouts or close wins may produce scores that do not accurately reflect athletes’ skills. To directly account for blowouts, [Harville \(2003\)](#) considers simple strategies such as capping margins of victory and adjusting extreme scores using hazard functions. In a non-sports setting, [Lenk and Tsai \(1990\)](#) proposes a DLM that uses a naive grid search to learn an appropriate Box-Cox transformation ([Box and Cox, 1964](#)) of the outcomes. While these methods are straightforward and intuitive, they lack the data-driven flexibility required for many real-world settings. [Xia *et al.* \(2000\)](#) considers the more flexible monotone spline transformation ([Ramsay, 1988](#)), albeit in the simpler setting of univariate autoregression with static parameters for an ecological time-series dataset. In this paper, we propose a Bayesian DLM with a monotone spline outcome transformation to rate athletes who compete in multi-competitor games with scored outcomes. Our model uses a Bayesian approach to learn the best transformation from the data in a principled manner while still preserving the efficiency and transparency of a standard DLM framework.

The paper proceeds as follows. Section 2 describes the general DLM framework and demonstrates the incorporation of monotone transformations into the

model. Section 3 describes an efficient model-fitting algorithm for the DLM with transformations. Finally, Section 4 compares our DLM to other candidate models for rating athletes in multi-competitor games, using data provided by the US Olympic and Paralympic Committee.

2. Model

We introduce the model proposed in this paper in two stages. First, we present a standard DLM framework for rating athletes. We then modify it to account for game effects and non-normal outcomes, and address the special case of head-to-head games.

2.1. Standard DLM for athlete rating

A standard DLM for rating athletes models each athlete’s observed scores as normally distributed around their latent ability, which evolves over time. The model likelihood for the score observed from a single athlete competing during time t takes the form:

$$p(y_t | \theta_t, \sigma^2) = N(\theta_t, \sigma^2), \quad (1)$$

where y_t is the observed score, θ_t is the athlete’s latent ability parameter at time t , and σ^2 is the observation variance. In this paper, we allow the latent ability parameter to evolve between time points as a normal random walk:

$$p(\theta_{t+1} | \theta_t, \sigma^2, w) = N(\theta_t, \sigma^2 w), \quad (2)$$

where w is an additional parameter that controls how much latent abilities may vary over time relative to the observation variance. Other stochastic processes may also be considered for the evolution of latent ability parameters, such as a mean-preserving random walk (Glickman and Hennessy, 2015) or an autoregressive process (Glickman and Stern, 1998). Unlike these other stochastic processes, the normal random walk diverges over time; in practice, however, data are typically modelled over relatively few time points in practice, so this phenomenon does not pose practical problems.

In a general sporting setting, we divide time into discrete *rating periods*, e.g., six-month sporting seasons, with multiple games within each rating period and multiple athletes within each game. Let p denote the total number of athletes in the data. Let T denote the total number of discrete rating periods, indexed by $t = 1, \dots, T$. Athletes may compete in any number of games within each rating period. Finally, let n_t denote the total number of observed scores within rating period t .

The data model (Equation 1) and innovation model (Equation 2) may now be rewritten in multivariate form as:

$$\begin{aligned} p(\mathbf{y}_t | \boldsymbol{\theta}_t, \sigma^2) &= N(X_t \boldsymbol{\theta}_t, \sigma^2 I_{n_t}) \\ p(\boldsymbol{\theta}_{t+1} | \boldsymbol{\theta}_t, \sigma^2, w) &= N(\boldsymbol{\theta}_t, \sigma^2 w I_p). \end{aligned}$$

Here, \mathbf{y}_t is the $n_t \times 1$ column vector of observed scores, $\boldsymbol{\theta}_t$ is the $p \times 1$ column vector of athlete latent abilities for rating period t , and I_k denotes the $k \times k$ identity matrix. The $n_t \times p$ model matrix X_t simply matches each athlete’s observed score(s) to their latent ability.¹ Note that athletes’ latent abilities are assumed to be constant within each rating period t , but may vary between rating periods t and $t + 1$.

2.2. Addressing game effects

In practice, athlete-rating DLMS need to account for conditions that affect game scores in a manner unrelated to latent athlete abilities. For example, a hot day might make all athletes in a race run more slowly, but the increased race times do not indicate weaker athletes. One approach to incorporate game-specific variation is to assume game-specific intercepts as part of the outcome model. This approach has been used, for example, by [Glickman and Stern \(1998\)](#).

Instead of assuming game-specific intercepts, we pre-process the data by subtracting game-specific means from the observed scores. This approach avoids concerns relating to the arbitrary specification of priors for the intercepts, which could affect downstream results. Each game-centered score \tilde{y} may then be modeled either by directly using Equation 1, or by using a game-centered latent ability, as:

$$p(\tilde{y} \mid \boldsymbol{\theta}_t, \sigma^2) = N(\theta_t - \bar{\theta}_{tg}, \sigma^2).$$

The value $\bar{\theta}_{tg}$ denotes the average latent ability across all of the players in game g within rating period t . Subtracting $\bar{\theta}_{tg}$ from each athlete’s latent ability adjusts for the fact that competing against a stronger pool of opponents in a game naturally results in worse scores relative to the competition.

To simplify notation for vector of game-centered scores $\tilde{\mathbf{y}}_t$, we write:

$$p(\tilde{\mathbf{y}}_t \mid \boldsymbol{\theta}_t, \sigma^2) = N(\bar{X}_t \boldsymbol{\theta}_t, \sigma^2 I_{n_t}), \quad (3)$$

where $\tilde{\mathbf{y}}_t \equiv \begin{bmatrix} \tilde{y}_{t1} \\ \vdots \\ \tilde{y}_{tg} \end{bmatrix}$ and $\bar{X}_t \equiv \begin{bmatrix} H_{n_{t1}} X_{t1} \\ \vdots \\ H_{n_{tg}} X_{tg} \end{bmatrix}$ for centering matrices $H_k \equiv I_k - \mathbf{1}_k \mathbf{1}_k^T$. For games $g = 1, \dots, g_t$ within rating period t , the $n_g \times 1$ vector of scores and $n_g \times p$ model matrix for game g are written as $\tilde{\mathbf{y}}_{tg}$ and X_{tg} , respectively.

2.3. Addressing non-normal outcomes

In many games, we might also suspect that athletes’ game-centered scores are not normally distributed around their game-centered latent abilities as assumed by Equation 3. Instead, we may assume that some transformation of the athletes’

¹Temporarily suppressing the time subscript t , the matrix X has a single nonzero entry per row. Per row r , if entry r of the column vector \mathbf{y} corresponds to a score earned by athlete a , then X_{ra} is set to equal 1.

scores is normally distributed around their latent abilities, so that the resulting model for transformed outcomes is:

$$p(\tau_{\lambda}(\tilde{\mathbf{y}}_t) \mid \boldsymbol{\theta}_t, \sigma^2, \boldsymbol{\lambda}) = N(\bar{X}_t \boldsymbol{\theta}_t, \sigma^2 I_{n_t}).$$

The transformation $\tau_{\lambda}(\cdot)$ is a function parameterized by a vector-valued parameter $\boldsymbol{\lambda}$.

In this paper, we use the monotone spline transformation from [Ramsay \(1988\)](#), but any monotone transformation with a computable Jacobian would work as well. The monotone spline transformation is a polynomial spline built from an I-spline basis (see [Ramsay \(1988\)](#) for more detail). For a given polynomial order d and knot sequence \mathbf{k} , an I-spline basis consists of B fixed, monotonically increasing basis functions $I_b(y \mid d, \mathbf{k})$, $b = 1, \dots, B$. The monotone spline transformation is then constructed as a linear combination of these basis functions:

$$\tau_{\boldsymbol{\lambda}}^{MS}(y) = \lambda_0 + \sum_{b=1}^B \lambda_b I_b(y \mid d, \mathbf{k}),$$

where λ_0 represents an intercept term and $\lambda_1, \dots, \lambda_B$ determine the shape of the transformation. We treat λ_0 as fixed, and define the transformation parameter $\boldsymbol{\lambda}$ as $\boldsymbol{\lambda} \equiv [\lambda_1 \dots \lambda_B]^T$. Note that because each basis function $I_b(\cdot)$ is monotone increasing, constraining the parameters $\lambda_1, \dots, \lambda_B$ to be non-negative ensures that the resulting spline transformation is also monotone increasing. Also, the sum $\sum_{b=1}^B \lambda_b$ determines the range of the monotone spline transformation function, so we constrain it to equal a constant c for identifiability.

2.4. Full Bayesian model

The full DLM with transformations is therefore as follows:

$$p(\boldsymbol{\psi}_t \mid \boldsymbol{\theta}_t, \sigma^2, \boldsymbol{\lambda}) = N(\bar{X}_t \boldsymbol{\theta}_t, \sigma^2 I_{n_t}) \quad (4)$$

$$p(\boldsymbol{\theta}_{t+1} \mid \boldsymbol{\theta}_t, \sigma^2, w) = N(\boldsymbol{\theta}_t, \sigma^2 w I_p), \quad (5)$$

where we define $\boldsymbol{\psi}_t \equiv \tau_{\boldsymbol{\lambda}}(\tilde{\mathbf{y}}_t)$, the transformed, game-centered observations, suppressing dependence on $\boldsymbol{\lambda}$ to simplify notation. To complete the model specification, we specify prior distributions for $\boldsymbol{\theta}_1$, σ^2 , w , and $\boldsymbol{\lambda}$:

$$\begin{aligned} p(\boldsymbol{\theta}_1 \mid \sigma^2, v_0) &= N(0, \sigma^2 v_0 I_p) \\ p(\sigma^2) &= \text{Inv-Gamma}(a_0, b_0) \\ p(w) &= \text{Half-Normal}(s_w^2) \\ p(\boldsymbol{\lambda}) &= c \cdot \text{Dirichlet}(\boldsymbol{\alpha}). \end{aligned}$$

The hyperparameters v_0 , a_0 , b_0 , s_w , c , and $\boldsymbol{\alpha}$ may be set to reflect prior beliefs about $\boldsymbol{\theta}_1$, σ^2 , w , and $\boldsymbol{\lambda}$. In the absence of available prior information, we set $v_0 = 10$, $a_0 = b_0 = 0.1$, and $s_w = 1$ to keep the priors fairly uninformative

about θ_1 , σ^2 , and w (Gelman *et al.*, 1995). We set α to be proportional to the λ parameters corresponding to the identity transformation, but keep $\sum_{b=1}^B \alpha_b = 1$ to keep the prior diffuse. If more shrinkage toward the identity transformation is desired, $\sum_{b=1}^B \alpha_b$ can be set to a higher value. Finally, we set λ_0 to equal the lowest score in the data and c to equal the range of the scores in the data so that the learned transformation roughly preserves the scale of the original data.

The Dirichlet prior on λ constrains the transformation parameter λ to have nonnegative components that sum to c . In practice, we find that using a weakly regularizing unconstrained prior for λ often results in better performance:

$$p(\lambda_b) = N^+(\alpha_b, s_\lambda^2) \text{ for } b = 1, \dots, B,$$

where N^+ indicates a normal distribution truncated below at 0. Theoretically, the shape of the monotone spline transformation is unidentifiable without a constraint on $\sum_{b=1}^B \lambda_b$; empirically, the mild regularization induced by the truncated normal priors effectively addresses these concerns. For this unconstrained model, we set α equal to the λ parameters corresponding to the identity transformation and control shrinkage toward the identity transformation using s_λ^2 . To allow maximum flexibility, we typically set s_λ^2 to a large value.

Figure 1 displays the graphical model representing the relationships between the model parameters $\{\theta_t\}_{t=1,\dots,T}$, σ^2 , w , and λ and the transformed data $\{\psi_t\}_{t=1,\dots,T}$. Figure 1 displays the conditional independences implied by Equations

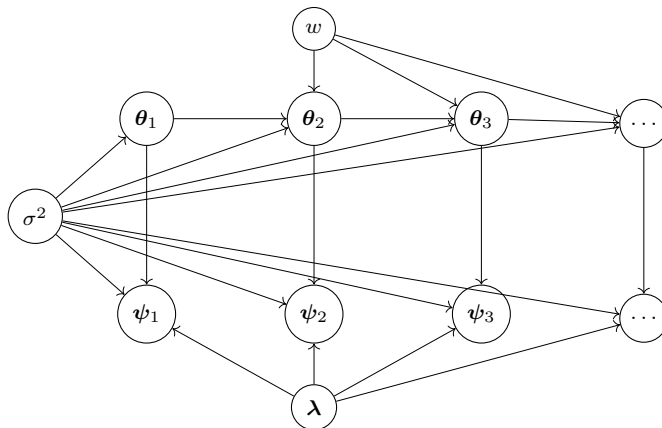


FIG 1. Graphical model for DLM with transformations

tions 4 and 5, which allow us to factor the joint distribution of our untransformed data and model parameters as:

$$p(\mathbf{y}_{1:T}, \boldsymbol{\theta}_{1:T}, \sigma^2, w, \boldsymbol{\lambda}) = J(\boldsymbol{\psi}_{1:T} \rightarrow \mathbf{y}_{1:T}) \times p(\sigma^2)p(w)p(\boldsymbol{\lambda}) \times \prod_{t=1}^T p(\psi_t | \boldsymbol{\theta}_t, \sigma^2, \boldsymbol{\lambda}) \times \prod_{t=1}^T p(\boldsymbol{\theta}_t | \boldsymbol{\theta}_{t-1}, \sigma^2, w),$$

where $J(\psi_{1:T} \rightarrow \mathbf{y}_{1:T})$ is the Jacobian of the inverse transformation, $\tau_{\boldsymbol{\lambda}}^{-1}(\cdot)$. The Jacobian term is vital to appropriately account for how the transformation rescales the data. For example, the Jacobian of the inverse monotone spline transformation is:

$$J^{MS}(\psi \rightarrow y) = \sum_{b=1}^B \lambda_b M_b(y | d, \mathbf{k}).$$

The I-spline basis functions used for the monotone spline are constructed by integrating M-spline basis functions; here, $M_b(\cdot)$ are the M-spline basis functions corresponding to their respective I-splines. Figure 2 displays the seven spline basis functions constructed for the biathlon relay training dataset we study in Section 4. Figure 2 shows how each I-spline basis function is constructed as the integral of an M-spline basis function.

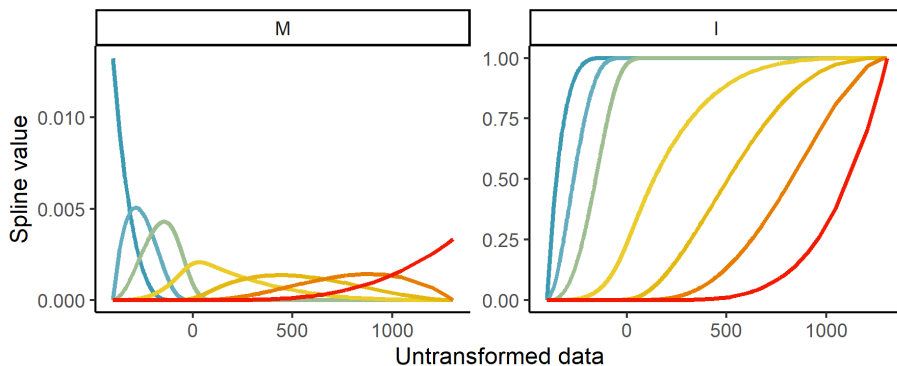


FIG 2. *Spline basis functions for biathlon relay training set*

2.5. Head-to-head games

While the general multi-competitor setup introduced above can be used for games with any number of players, we introduce a slightly simpler setup for the special case of head-to-head games. In head-to-head games, it is generally more natural to consider monotone transformations of score differences, which have no direct analogues in the multi-competitor setting. Instead of modeling the $2g_t \times 1$ vector of athlete scores \mathbf{y}_t , we can model the $g_t \times 1$ vector of score differences \mathbf{z}_t , where we subtract the second athlete's score from the first athlete's score. The resulting model likelihood is:

$$p(\tau_{\boldsymbol{\lambda}}(\mathbf{z}_t) | \boldsymbol{\theta}_t, \sigma^2, \boldsymbol{\lambda}) = N(Z_t \boldsymbol{\theta}_t, \sigma^2 I_{n_t}).$$

Note that we have simply replaced the model matrix \bar{X}_t with the model matrix Z_t , which is defined as a matrix with two nonzero entries per row: 1 in the

column corresponding to the first athlete and -1 in the column corresponding to the second athlete. The observed score difference is taken as the first athlete's score minus the second athlete's score.

3. Model fitting

3.1. Model-fitting procedure

We estimate the model parameters $(\boldsymbol{\theta}_{1:T}, \sigma^2, w, \boldsymbol{\lambda})$ via a two-step procedure. In our application of interest, we would like to be able to quickly update athlete ratings (i.e., latent ability estimates) shortly after the results from a game. While we could estimate the full posterior distribution of all of the model parameters after each game, this may be a slow and computationally expensive process. Instead, we fit the model using the following procedure:

1. Estimate w and $\boldsymbol{\lambda}$: using a training subset consisting of the first T_{train} rating periods in the dataset, obtain estimates \hat{w} and $\hat{\boldsymbol{\lambda}}$.
2. Estimate $\boldsymbol{\theta}_{1:T}$ and σ^2 : given \hat{w} and $\hat{\boldsymbol{\lambda}}$, use the full dataset to obtain estimates $\hat{\boldsymbol{\theta}}_{1:T}$ and $\hat{\sigma}^2$.

While step 1 is computationally expensive, step 2 can be accomplished quickly using standard Kalman filter updates, as will be described later in this section. When the results from a new game become available, we can just run step 2 using the previously learned values of \hat{w} and $\hat{\boldsymbol{\lambda}}$ to quickly update ratings.

The marginal posterior density of w and $\boldsymbol{\lambda}$ can be expressed in closed form (up to a normalizing constant) as:

$$p(w, \boldsymbol{\lambda} \mid \mathbf{y}_{1:T_{train}}) \\ \propto J(\boldsymbol{\psi}_{1:T_{train}} \rightarrow \mathbf{y}_{1:T_{train}}) p(w) p(\boldsymbol{\lambda}) \prod_{t=1}^{T_{train}} p(\boldsymbol{\psi}_t \mid \boldsymbol{\psi}_{1:t-1}, w, \boldsymbol{\lambda})$$

for the priors on w and $\boldsymbol{\lambda}$ and posterior predictive densities:

$$p(\boldsymbol{\psi}_t \mid \boldsymbol{\psi}_{1:t-1}, w, \boldsymbol{\lambda}) = t_{2a_{t-1}}(\bar{X}_t \mathbf{m}_{t-1}, \frac{b_{t-1}}{a_{t-1}} [I_{n_t} + \bar{X}_t (V_{t-1} + wI_p) \bar{X}_t^T]),$$

where \mathbf{m}_t , V_t , a_t , and b_t are computed using standard Kalman filter equations on the transformed data (Särkkä, 2013):

$$\begin{aligned} V_t &= ((V_{t-1} + wI_p)^{-1} + \bar{X}_t^T \bar{X}_t)^{-1} \\ \mathbf{m}_t &= V_t ((V_{t-1} + wI_p)^{-1} \mathbf{m}_{t-1} + \bar{X}_t^T \boldsymbol{\psi}_t) \\ a_t &= a_{t-1} + \frac{1}{2} n_t \\ b_t &= b_{t-1} + \frac{1}{2} [\mathbf{m}_{t-1}^T (V_{t-1} + wI_p)^{-1} \mathbf{m}_{t-1} + \boldsymbol{\psi}_t^T \boldsymbol{\psi}_t - \mathbf{m}_{t-1}^T V_{t-1}^{-1} \mathbf{m}_{t-1}] \\ &= b_{t-1} + \frac{1}{2} (\boldsymbol{\psi}_t - \bar{X}_t \mathbf{m}_{t-1})^T (I_{n_t} + \bar{X}_t (V_{t-1} + wI_p) \bar{X}_t^T)^{-1} (\boldsymbol{\psi}_t - \bar{X}_t \mathbf{m}_{t-1}). \end{aligned}$$

We can obtain samples of w and $\boldsymbol{\lambda}$ from $p(w, \boldsymbol{\lambda} \mid \mathbf{y}_{1:T_{\text{train}}})$ using standard Markov Chain Monte Carlo (MCMC) methods. We implement our model in Stan, which uses Hamiltonian Monte Carlo.

In practice, we can instead take a maximum a posteriori (MAP) approach using standard optimization routines to greatly reduce the computational burden. For most applications, we are only interested in estimating reasonable values for w and $\boldsymbol{\lambda}$, not in conducting full Bayesian inference on them; as such, it often makes sense to simply find the posterior mode of $p(w, \boldsymbol{\lambda} \mid \mathbf{y}_{1:T_{\text{train}}})$. Importantly, integrating $\boldsymbol{\theta}_{1:T_{\text{train}}}$ and σ^2 out of the posterior instead of maximizing $p(w, \boldsymbol{\lambda}, \boldsymbol{\theta}_{1:T_{\text{train}}}, \sigma^2 \mid \mathbf{y}_{1:T_{\text{train}}})$ with respect to each parameter produces a better-informed posterior mode of w and $\boldsymbol{\lambda}$.

Any nonlinear optimization algorithm can be used to obtain MAP estimates. For the constrained optimization (with a Dirichlet prior on $\boldsymbol{\lambda}$), we choose to use the Augmented Lagrangian Adaptive Barrier Minimization Algorithm (Varadhan, 2015). For the unconstrained optimization (with normal priors on the λ_b parameters), we find that the Nelder-Mead algorithm (Nelder and Mead, 1965) generally gives the most stable results, though the L-BFGS algorithm (Liu and Nocedal, 1989) is much faster in practice. While these optimization-based approaches may theoretically get stuck in local modes, we find that in practice they produce reasonable and effective results.

Given the MAP estimate $(\hat{w}, \hat{\boldsymbol{\lambda}})$, we can finally estimate the posterior distributions of $\{\boldsymbol{\theta}\}_{t=1, \dots, T}$ and σ^2 by transforming the full dataset using $t_{\hat{\boldsymbol{\lambda}}}(\cdot)$ and running the Kalman filter equations using \hat{w} . Full implementation details can be found in Appendix A.

3.2. Smoothing

The Kalman filter equations produce estimates of the filtered latent ability parameter distributions $p(\boldsymbol{\theta}_t \mid \boldsymbol{\psi}_{1:t}, \sigma^2, \boldsymbol{\lambda})$. In the second stage of the model-fitting procedure, we may also wish to calculate the smoothed latent ability parameter distributions $p(\boldsymbol{\theta}_t \mid \boldsymbol{\psi}_{1:T}, \sigma^2, \boldsymbol{\lambda})$, where the full dataset informs each latent ability parameter estimate. The Rauch-Tung-Striebel smoother (Särkkä, 2013) provides a simple algorithm for doing so. We can compute the smoother updates as:

$$p(\boldsymbol{\theta}_t \mid \boldsymbol{\psi}_{1:T}, \sigma^2, \boldsymbol{\lambda}) = N(\mathbf{m}_t^s, \sigma^2 V_t^s)$$

for:

$$\begin{aligned} \mathbf{m}_t^s &= \mathbf{m}_t + S_t(\mathbf{m}_{t+1}^s - \mathbf{m}_t) \\ V_t^s &= V_t + S_t(V_{t+1}^s - V_t - wI)S_t^T \end{aligned}$$

for scaling matrix $S_t = V_t(V_t + wI)^{-1}$, where the \mathbf{m}_t and V_t values are the original \mathbf{m}_t and V_t values computed using the Kalman filter equations. The smoother updates are computed starting from rating period $t = T$ backwards to rating period $t = 1$, starting from $\mathbf{m}_T^s = \mathbf{m}_T$ and $V_T^s = V_T$.

4. Empirical results

4.1. USOPC athletic data

We illustrate our model on a variety of Olympic sport datasets provided to us by the US Olympic and Paralympic Committee. The data roughly span from 2004 to 2019 and include the score outcomes from selected national and international competitions. We briefly describe each dataset below.

Biathlon The biathlon data come from the men’s 20km individual biathlon and the men’s 4×7.5 km relay. In the 20km biathlon, athletes ski a cross-country track between four rifle-shooting rounds. In each shooting round, they shoot at five targets. Each miss incurs a penalty, which may be extra time added or a penalty skiing lap, depending on the particular race’s rules. The biathlon relay is similar, with two shooting rounds per relay leg. In both competitions, athletes compete to finish the race as quickly as possible, so we use each athlete’s total time (in seconds) as their score.

Diving The diving data come from women’s 3m springboard. In diving competitions, athletes receive scores for each of their dives in a round. After each round of diving, only the top-scoring athletes may qualify for the next round.

Our dataset includes the total cumulative scores for athletes who compete in the final round, but only includes the relative rankings for athletes who are eliminated in earlier rounds. To try to make use of the full dataset, we naively impute scores for the eliminated athletes by assigning scores evenly spaced between zero and the minimum score in the final round, based the relative rankings. For example, if five athletes miss the final round, and the minimum score in the final round is 100, we would assign scores of 0, 20, 40, 60, and 80 to the five athletes, in order of their relative rankings.

Fencing The fencing data come from women’s sabre fencing. In each bout, the first athlete to score fifteen points wins. We record the score difference between the two athletes as the outcome of each game.

Rugby The rugby data come from men’s rugby sevens. We record the score difference between the two teams as the outcome of each game.

4.2. Model fitting and validation

We fit our unconstrained model to the biathlon, biathlon relay, diving, fencing, and rugby datasets. For the multicompetitor sports (biathlon, biathlon relay, diving), we divide the sixteen years of data into six-month-long rating periods. The head-to-head sports (fencing, rugby) naturally have more games, so we divide them into roughly three-month-long rating periods. Choosing a shorter rating period allows more flexibility for athlete abilities to change, but reduces the number of games that can be used to infer abilities within the rating period.

We conduct full MCMC (four chains, 1000 burn-in iterations, 1000 samples) as well as MAP estimation using the Nelder-Mead and L-BFGS optimization algorithms. To assess the convergence of our MCMC estimates of the posterior distributions of w and λ , we check trace plots and the \hat{R} diagnostic for Hamiltonian Monte Carlo. Visual inspection of the trace plots does not suggest any evidence of non-convergence, and \hat{R} is nearly equal to one for all model parameters. The Nelder-Mead and L-BFGS algorithms converge under default convergence tolerances.

Before examining the DLM results, we first confirm that the MAP estimates produce similar results as full MCMC. Figure 3 compares the posterior mean of the transformations learned using full MCMC to the transformations learned using MAP with the Nelder-Mead and L-BFGS algorithms. We see that the

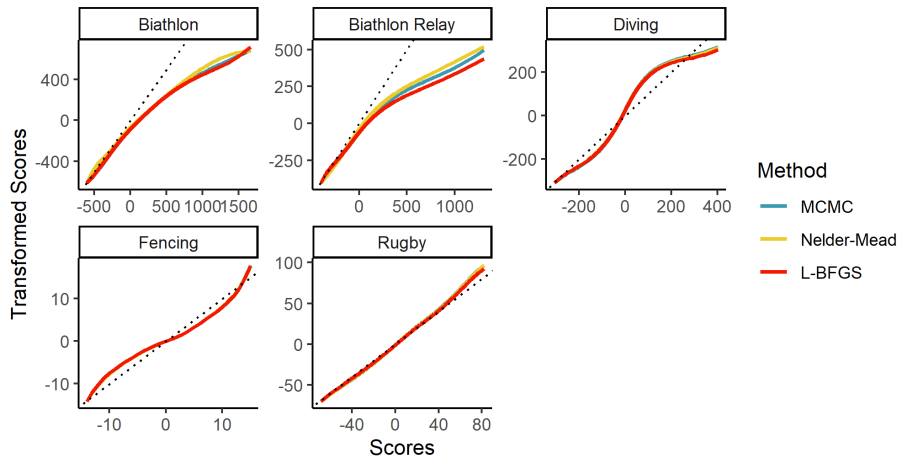


FIG 3. Comparison of algorithms for estimating λ . Dotted line represents the identity transformation, $y = x$.

learned transformations are essentially the same across all three algorithms for all five sports. The learned w parameters (not shown) are also very similar. As a result, using MAP methods rather than full MCMC does not significantly impact model performance, while it can lead to significant speedups. For example, for the biathlon dataset (~ 6000 observations from ~ 700 athletes over ~ 60 events), full MCMC took roughly 8 hours, but the Nelder-Mead optimization took only 30 minutes, and L-BFGS converged in less than one minute (all on a laptop with an Intel Core i7-8550U CPU). To simplify assessment, visualization, and discussion of our results, we will focus on the transformations estimated using full MCMC moving forward, though results are similar for the transformations estimated using MAP.

Next, we assess the fit of the DLM on our transformed datasets. To do so, we use the first two-third rating periods as a training set to learn an appropriate transformation and leave the last one-third rating periods as a test set.

We then visualize $(\psi_t - \bar{X}_t \mathbf{m}_{t-1})$, i.e., the one-step prediction residuals, on the test set. If the learned transformation is effective, the residuals should be approximately normally distributed. Figure 4 shows Q-Q plots of standardized test-set residuals against standard normal quantiles. While the residuals show

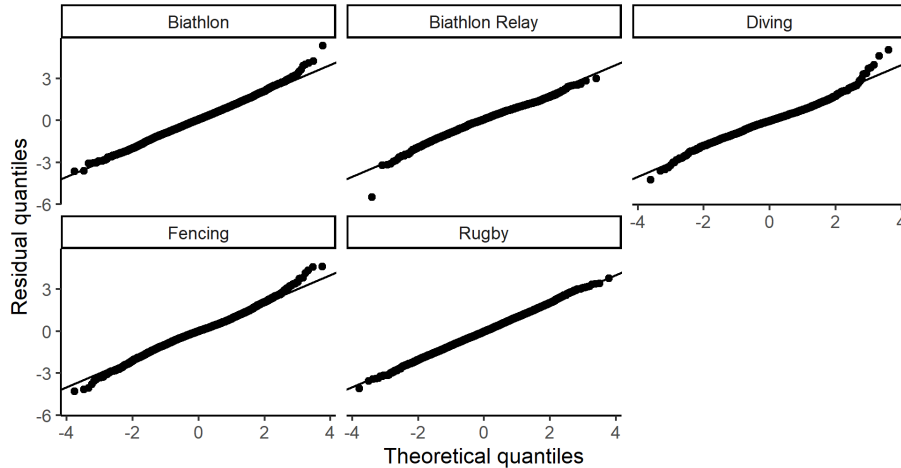


FIG 4. Q-Q plots of test-set residuals compared to standard normal quantiles

some slight outliers at the extremes, they are largely normally distributed. The learned transformations thus appear to produce reasonable fits of the standard DLM to these datasets.

4.3. Case studies: biathlon and rugby

We use the biathlon and rugby datasets to illustrate the results from our model. For both datasets, we learn an unconstrained monotone spline transformation using MCMC, transform the dataset, and run the Kalman filter on the transformed data.

Figure 5 shows the smoothed latent ability point estimates for the 25 biathletes with the most biathlons entered. In the biathlon, low race times are better, so negative ability parameters indicate strong athletes. Of the visualized latent ability trajectories, two stand out, and Figure 5 additionally shows their 90% confidence intervals. The trajectory in blue belongs to the “King of Biathlon,” Ole Einar Bjørndalen, the winningest biathlete of all time at the Olympics, Biathlon World Championships, and the Biathlon World Cup tour. Though the scope of our dataset does not include the start of his career in the 1990s, the model clearly notes his dominance in the early 2000s. The trajectory in red belongs to Martin Fourcade, who began serious international competition in 2008 and proceeded to put together a record-breaking string of seven overall World Cup titles in a row from 2011 to 2018. Bjørndalen and Fourcade are the

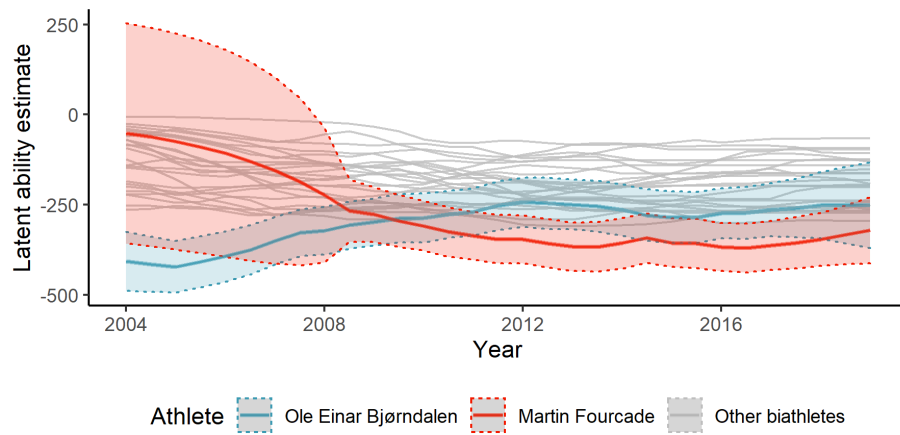


FIG 5. Smoothed estimated means of ability parameters of 25 biathletes with the most races entered, over time. 90% central posterior interval shown for Ole Einar Bjørndalen and Martin Fourcade.

two names considered in discussions of the greatest male biathlete of all time. Our model notes Fourcade’s quick rise to prominence, projecting that he would begin to outperform Bjørndalen as early as 2009, though interestingly it never projects Fourcade’s latent ability to exceed Bjørndalen’s peak latent ability in 2005.

Figure 6 shows the smoothed latent ability point estimates and corresponding 50% posterior intervals for the national rugby teams of Fiji, New Zealand, and South Africa, three countries popularly known for their strong rugby teams. Here, more positive latent ability estimates represent stronger teams. While the three teams have similar estimated strengths during the time span of the data, we see that New Zealand enjoyed a brief stretch of relative dominance from roughly 2007-2013.

4.4. Model results

Another result of interest is the monotone spline transformation learned by the DLM with transformations. Figure 7 displays 100 posterior transformation samples for each of the five sports, under the unconstrained optimization. The transformations generally reflect conventional wisdom about scores from these sports. For example, we sometimes see very slow race times in the biathlon and biathlon relay, which occur when an athlete makes a few shooting mistakes and takes penalties. We expect to see a negative feedback loop in the biathlon where taking penalties causes athletes to get more frustrated or tired from penalty laps, which causes more penalties. This means that extremely slow race times may not reflect extremely poor skill. The learned transformation shrinks the very slow race times to be less extreme, which intuitively helps to make them better

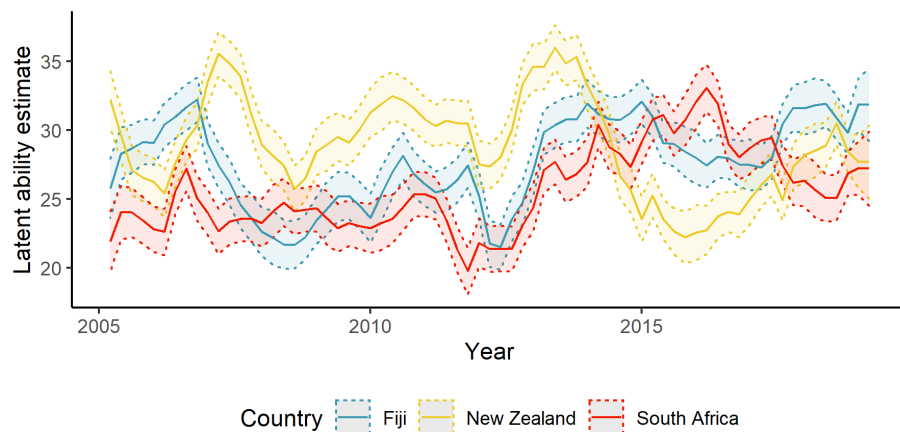


FIG 6. Smoothed estimated means of ability parameters and 50% central posterior intervals shown for Fiji, New Zealand, and South Africa national teams.

reflect athlete skill in the normal DLM. On the other hand, the transformation learned for fencing magnifies extreme score differences. In a fencing bout, points are scored one-at-a-time; after each touch (i.e., point scored), the fencers reset to their starting positions. This makes very one-sided matches relatively rare, since even outmatched fencers can typically score some number of lucky points in a match to fifteen points. The transformation notes this and indicates that when a fencer wins by many points, they are much stronger than their opponent, even more so than the large score gap may suggest.

Table 4.4 shows the posterior means of the \sqrt{w} and σ parameters for each of the five sports. Recall that σ^2 represents the observation variance and w represents the ratio of the innovation variance to the observation variance, so σ and $\sigma \cdot \sqrt{w}$ would represent the observation and innovation standard deviations, respectively. For example, in the biathlon data, the model estimates that the innovation standard deviation is approximately 28% as large as the observation standard deviation of 114.7. Note that the σ values are on the scale of the transformed data, rather than the original scale of the data.

Sport	\sqrt{w}	σ
Biathlon	0.28	114.7
Biathlon relay	0.26	79.0
Diving	0.24	58.5
Fencing	0.07	3.2
Rugby	0.18	14.7

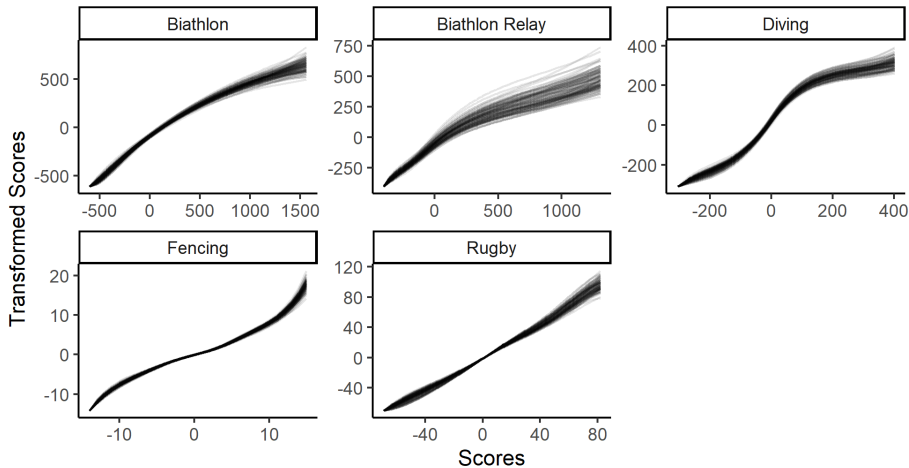


FIG 7. Transformations learned by DLM with transformations

4.5. Comparing rating methods

To evaluate the DLM with transformations, we compared the accuracy of its predictions to predictions made by other models for multi-competitor and head-to-head athlete rating. For multi-competitor sports, we compared the DLM with transformations (LM-T) to the DLM without transformations (LM) and the dynamic rank-order logit model (ROL) from [Glickman and Hennessy \(2015\)](#). For head-to-head sports, we compare to the Glicko rating system (GLO; [Glickman, 1999](#)). We use the first two-third rating periods in each dataset as a training set to tune the model hyperparameters w and λ , fit the model on the full dataset, and finally evaluate its predictions for the test set (i.e., the last one-third rating periods). For multi-competitor games, we evaluate predictions using the Spearman correlations between the observed and predicted athlete rankings in each game. This approach was taken in [Glickman and Hennessy \(2015\)](#) to evaluate predictability on a test set. We summarize these game correlations ρ_{tg} over the test set using a game-size-weighted average ([Glickman and Hennessy, 2015](#)):

$$\rho = \frac{\sum_{t=\lceil \frac{2}{3}T \rceil}^T \sum_{g=1}^{g_t} (n_{tg} - 1) \rho_{gt}}{\sum_{t=\lceil \frac{2}{3}T \rceil}^T \sum_{g=1}^{g_t} (n_{tg} - 1)}. \quad (6)$$

Note that we limit ourselves to using rank-based metrics to facilitate comparison with the ROL model, which predicts athlete ranking probabilities rather than scores. For head-to-head games, we evaluate predictions using the average accuracy of winner predictions in the test set.

Tables 1 and 2 show the weighted Spearman correlation (Equation 6) of the ranking predictions for the multi-competitor sports and the accuracy of winner/loser predictions for the head-to-head sports.

	Model		
Sport	LM-T	LM	ROL
Biathlon	.64	.61	.61
Biathlon Relay	.77	.75	.75
Diving	.64	.62	.61

TABLE 1

Weighted spearman correlations of predictions

	Model		
Sport	LM-T	LM	GLO
Fencing	.70	.67	.68
Rugby	.72	.72	.70

TABLE 2

Accuracy of winner predictions

Across the five datasets, we see some evidence that the LM-T model outperforms the other models in terms of predictive performance. While it is difficult to generally evaluate the relative empirical performance of the LM-T model with only five datasets, we see that it improves predictive accuracy across nearly all of the datasets. The only exception is the rugby dataset, where the LM-T model essentially learns an identity transformation, so we would not expect it to outperform the LM model. The results of athletic competitions are generally challenging to predict; small improvements in predictive performance can therefore be fairly valuable for generating a competitive edge.

5. Discussion

In this paper, we introduce a novel model to rate athletes who compete in head-to-head and multi-competitor sports with score outcomes. Using observed scores rather than rankings to rate athletes provides additional information, which generally improves predictions in the settings we consider. We can fit the model either using MCMC or an MAP approach, both which utilize the computational efficiency of the Kalman filter to learn an appropriate transformation to apply to the score outcomes.

The simple normal DLM at the core of our model makes a variety of extensions possible. For example, we choose to use a normal random walk as the innovation process for athletes' latent abilities, which may easily be replaced by alternative innovation processes, such as a mean-preserving random walk (Glickman and Hennessy, 2015) or an autoregressive process (Glickman and Stern, 1998). Also, external covariates related to athletes (e.g., height, age, experience), events (e.g., weather conditions), and/or other factors may be assigned fixed or time-varying coefficients and straightforwardly incorporated into the normal likelihood and innovation equations. If transforming outcomes to normality is infeasible in a particular setting, the normal likelihood could be also extended to the likelihood of a generalized linear model (West, Harrison and Migon, 1985).

While we focus on athlete rating, our model may be used for a wide range of different problems. Dynamic linear models are very popular for analyzing time series data in fields ranging from economics and finance to health and ecology. In many of these applications, the normal likelihood in a standard normal DLM may be misspecified, which can be addressed by learning an order-preserving monotone transformation using the model introduced in this paper.

The problem of athlete rating has interested organizations and individuals alike for many years. Appropriately using the information contained in game scores is an important but challenging task, due to the unusual features of score information in different games. This paper provides a general method to address these challenges, which can be applied to a wide range of multi-competitor and head-to-head games.

Acknowledgements

We thank Dan Webb at the U.S. Olympic and Paralympic Committee for providing the data for this work. This research was supported in part by a research contract from the U.S. Olympic and Paralympic Committee, and by the National Science Foundation Graduate Research Fellowship Program under Grant No. DGE1745303.

References

- BAKER, R. D. and MCHALE, I. G. (2015a). Deterministic evolution of strength in multiple comparisons models: who is the greatest golfer? *Scandinavian Journal of Statistics* **42** 180–196.
- BAKER, R. D. and MCHALE, I. G. (2015b). Time varying ratings in association football: the all-time greatest team is... *Journal of the Royal Statistical Society. Series A (Statistics in Society)* 481–492.
- BOX, G. E. and COX, D. R. (1964). An analysis of transformations. *Journal of the Royal Statistical Society: Series B (Methodological)* **26** 211–243.
- CARON, F. and TEH, Y. W. (2012). Bayesian nonparametric models for ranked data. *arXiv preprint arXiv:1211.4321*.
- CATTELAN, M., VARIN, C. and FIRTH, D. (2013). Dynamic Bradley–Terry modelling of sports tournaments. *Journal of the Royal Statistical Society: Series C (Applied Statistics)* **62** 135–150.
- GELMAN, A., CARLIN, J. B., STERN, H. S. and RUBIN, D. B. (1995). *Bayesian data analysis*. Chapman and Hall/CRC.
- GLICKMAN, M. E. (1999). Parameter estimation in large dynamic paired comparison experiments. *Journal of the Royal Statistical Society: Series C (Applied Statistics)* **48** 377–394.
- GLICKMAN, M. E. (2001). Dynamic paired comparison models with stochastic variances. *Journal of Applied Statistics* **28** 673–689.
- GLICKMAN, M. E. and HENNESSY, J. (2015). A stochastic rank ordered logit model for rating multi-competitor games and sports. *Journal of Quantitative Analysis in Sports* **11** 131–144.

- GLICKMAN, M. E. and STERN, H. S. (1998). A state-space model for National Football League scores. *Journal of the American Statistical Association* **93** 25–35.
- HARVILLE, D. (1977). The use of linear-model methodology to rate high school or college football teams. *Journal of the American Statistical Association* **72** 278–289.
- HARVILLE, D. A. (2003). The selection or seeding of college basketball or football teams for postseason competition. *Journal of the American Statistical Association* **98** 17–27.
- HERBRICH, R., MINKA, T. and GRAEPEL, T. (2006). Trueskill™: A Bayesian skill rating system. In *Proceedings of the 19th international conference on neural information processing systems* 569–576.
- INGRAM, M. (2019). A point-based Bayesian hierarchical model to predict the outcome of tennis matches. *Journal of Quantitative Analysis in Sports* **15** 313–325.
- KOVALCHIK, S. (2020). Extension of the Elo rating system to margin of victory. *International Journal of Forecasting* **36** 1329–1341.
- LENK, P. J. and TSAI, C.-L. (1990). Transformations and dynamic linear models. *Journal of Forecasting* **9** 219–232.
- LIU, D. C. and NOCEDAL, J. (1989). On the limited memory BFGS method for large scale optimization. *Mathematical programming* **45** 503–528.
- LOPEZ, M. J., MATTHEWS, G. J. and BAUMER, B. S. (2018). How often does the best team win? A unified approach to understanding randomness in North American sport. *The Annals of Applied Statistics* **12** 2483–2516.
- MCKEOUGH, K. (2020). A Tale of Two Multi-Phase Inference Applications PhD thesis, Harvard University.
- NELDER, J. A. and MEAD, R. (1965). A simplex method for function minimization. *The computer journal* **7** 308–313.
- PLACKETT, R. L. (1975). The analysis of permutations. *Journal of the Royal Statistical Society: Series C (Applied Statistics)* **24** 193–202.
- RAMSAY, J. O. (1988). Monotone Regression Splines in Action. *Statistical Science* **3** 425–441.
- SÄRKKÄ, S. (2013). *Bayesian filtering and smoothing* 3. Cambridge University Press.
- STAN DEVELOPMENT TEAM, (2021). RStan: the R interface to Stan. R package version 2.21.3.
- VARADHAN, R. (2015). alabama: Constrained Nonlinear Optimization R package version 2015.3-1.
- WANG, W. and YAN, J. (2021). Shape-Restricted Regression Splines with R Package splines2. *Journal of Data Science* **19** 498–517.
- WEST, M., HARRISON, P. J. and MIGON, H. S. (1985). Dynamic generalized linear models and Bayesian forecasting. *Journal of the American Statistical Association* **80** 73–83.
- XIA, Y., TONG, H., LI, W. K. and ZHU, L. X. (2000). On the estimation of an instantaneous transformation for time series. *Journal of the Royal Statistical Society: Series B (Statistical Methodology)* **62** 383–397.

YEO, I. and JOHNSON, R. A. (2000). A new family of power transformations to improve normality or symmetry. *Biometrika* **87** 954-959.

Appendix A: Model implementation details

We make a few minor changes to the model presented in section 3. We clear the off-diagonal elements of the V_t matrix between rating periods in the Kalman filter equations. This keeps the matrix operations relatively sparse, which speeds up computation time. The correlations between players induced by playing in the same games tend to be weak in any case, so this change does not hurt model performance. We also cap the diagonal entries of V_t at v_0 , assuming that we cannot be less certain about a player’s ability than we are before seeing any data. Appendix B contains a simulation study confirming that these approximations do not significantly hurt model performance.

We implement the monotone spline transformations using the `splines2` package in R (Wang and Yan, 2021). We consider splines of degree three, with three knots placed at the terciles of the raw centered data. We implement the Bayesian model using the `rstan` package in R (Stan Development Team, 2021), which uses Hamiltonian Monte Carlo to generate posterior samples. For MAP estimates, we primarily use the Nelder-Mead algorithm (Nelder and Mead, 1965) as implemented in the `optim()` function in R. The L-BFGS algorithm (Liu and Nocedal, 1989) is implemented via the `optimizing()` function in the `rstan` package.

Appendix B: Simulation study

In this paper, we make a number of approximations, as described in Appendix A. To confirm that these approximations do not significantly hurt performance, we validate our method using a few detailed simulation studies. In particular, we evaluate how well the LM-T model can recover the true data-generating parameters σ^2 , w , and λ . We also evaluate recovery of $\{\theta_t\}_{t=1,\dots,T}$ by evaluating predictive accuracy, and compare accuracy between the LM-T, LM, and ROL/GLO models.

We simulate data according to the data-generating process implied by the model:

1. **Set data size and data-generating parameters:** pick values for p , T , $\{g_t\}$, and $\{n_{tg}\}$; also, pick true values for v_0 , σ^2 , w , and λ for a true transformation $\tau_\lambda(\cdot)$.
2. **Generate athlete latent abilities:** draw $\theta_1 \sim N(0, \sigma^2 v_0)$ and $\theta_t \sim N(\theta_{t-1}, \sigma^2 w)$ for $t = 1, \dots, T$.
3. **Generate untransformed scores:** for each game g in rating period t , randomly sample n_{tg} athletes and generate untransformed scores as: $\psi_{tg} \sim N(\theta_{tg} - \theta_g, \sigma^2)$.
4. **Generate observed scores:** compute $\mathbf{y}_{tg} = t_\lambda^{-1}(\psi_{tg})$.

Note that while the simulated untransformed scores are not explicitly game-centered, their mean is zero within each game.

To evaluate parameter recovery and compare model predictions, we simulate 50 datasets for each of a variety of data-generating parameters. We fix $p = 100$ and $T = 20$, and consider $n_{tg} = 2, 10, \text{ and } 50$ to correspond to head-to-head games and small/large multi-competitor games. For each setting, we set g_t such that $n_{tg} * g_t$ equals a range of values from 20 to 250 to simulate low to high data environments. Finally, we fix $v_0 = 10$, $\sigma^2 = 100$, and $w = 0.5$, and we consider data-generating Yeo-Johnson transformations (Yeo and Johnson (2000)) with $\lambda = 0.7, 1, 1.3$ to see how well the DLM with transformations can recover transformations that shrink, preserve, and stretch the data.

After simulating the multi-competitor data, we run the LM-T model. We record its estimate of the hyperparameters (w, λ) and the posterior mean of σ^2 . We then run the LM and ROL models on each dataset and evaluate all three models' predictions.

B.1. Simulation results: parameter recovery

In this section, we verify that the LM-T model can accurately recover the data-generating parameters in multi-competitor games.

First, we verify that the LM-T model can accurately recover the λ parameter for the data-generating Yeo-Johnson transformation. Figure 8 plots the estimated value of λ against the number of multi-competitor games per rating period, aggregated across 50 simulations in each setting. The dotted lines represent the true data-generating value of λ . We see that λ recovery is generally

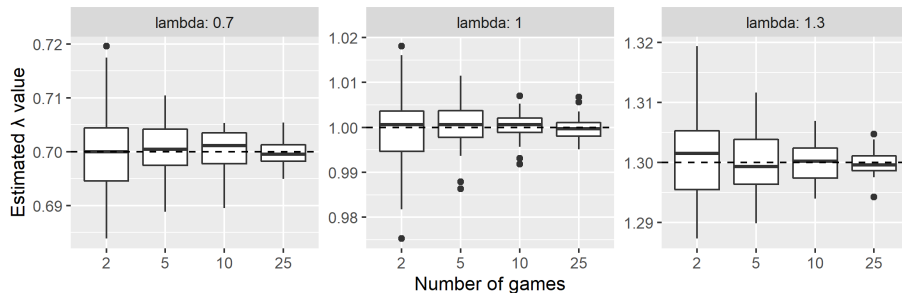


FIG 8. LM-T model recovery of λ . Dotted line represents the true data-generating λ parameter.

extremely accurate; even with only two ten-player games per rating period, the estimated value of λ is rarely more than 0.01 away from the true value of λ .

Figure 9 plots the value of w estimated by the LM-T model against the number of games per rating period, across 150 datasets.² We see that w recovery is

²We aggregate across the true λ values in the simulations, since results for w are qualitatively identical regardless of λ .

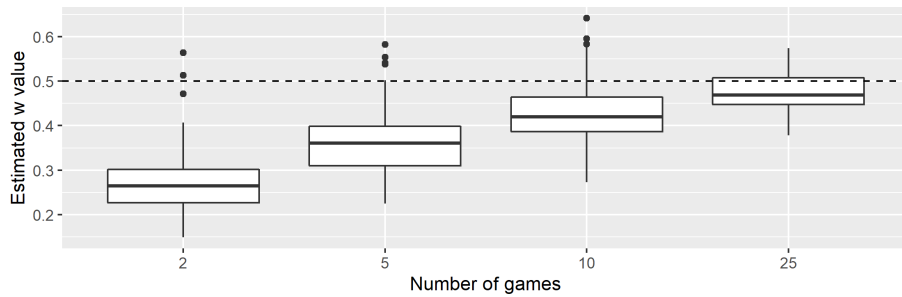


FIG 9. *LM-T model recovery of w . Dotted line represents the true data-generating w parameter.*

less accurate than λ recovery. The LM-T model generally underestimates w when there are few games, and only consistently recovers the true data-generating w with 25 ten-player games per rating period. This behavior is appropriate; when there are few games per rating period to accurately estimate player strengths, it makes sense to be more conservative when updating the estimates between rating periods, i.e., to have a lower w .

Similarly, Figure 10 plots the value of σ estimated by the LM-T model against the number of games per rating period, again across 150 datasets. We see that

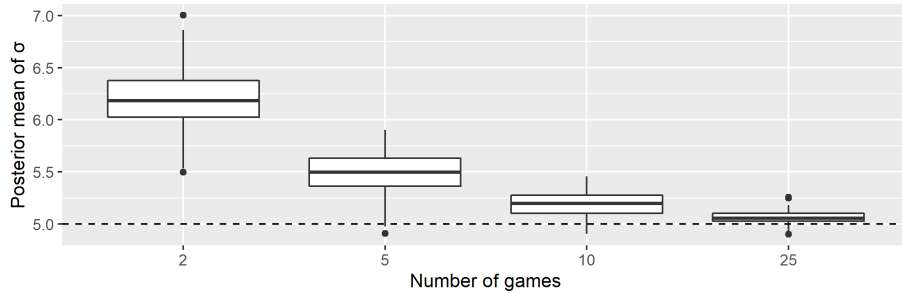


FIG 10. *LM-T model recovery of σ . Dotted line represents the true data-generating σ parameter.*

σ recovery is also less accurate than λ recovery for small data sizes, but that the behavior of the σ estimates is still appropriate. When there are few observations per rating period, we cannot be too certain of our estimated latent ability parameters within each rating period; this inflates our σ estimate (which in turn deflates our w estimate). Again, it makes sense for the model to be somewhat conservative when the data do not provide much information.

B.2. Simulation results: model comparisons

As a final check, we can visualize the performance of the LM-T model against the LM and ROL/GLO models for multi-competitor/head-to-head games. We would expect the LM-T model to perform very well for these data, since the data are simulated according to the data-generating process assumed by the LM-T model. Figure 11 plots the weighted spearman correlation of the observed rankings and the rankings predicted by the LM-T, LM, and ROL models against the number of games per rating period. When $\lambda = 1$, i.e., the transformation is

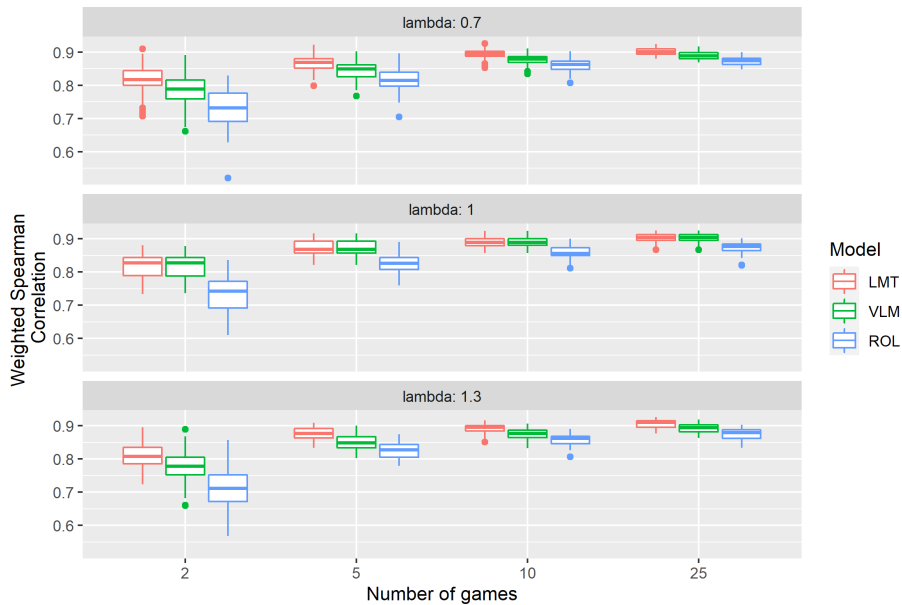


FIG 11. Predictive performance of LM-T, LM, and ROL models for multi-competitor data

the identity transformation, we see that the LM-T and LM models have nearly identical performances, as expected. Otherwise, the LM-T model outperforms the other two models, with differences in performance shrinking somewhat as the number of observed games per rating period increases.

Figure 12 plots the accuracy of head-to-head game winner predictions for the three models. Results are similar regardless of the data-generating λ value, so each boxplot aggregates over 150 simulations. For head-to-head games, the LM-T model and LM models perform similarly well. The head-to-head LM-T model assumes a slightly different data-generating process than what is used, so it is not surprising to see that it does not clearly outperform the other models.

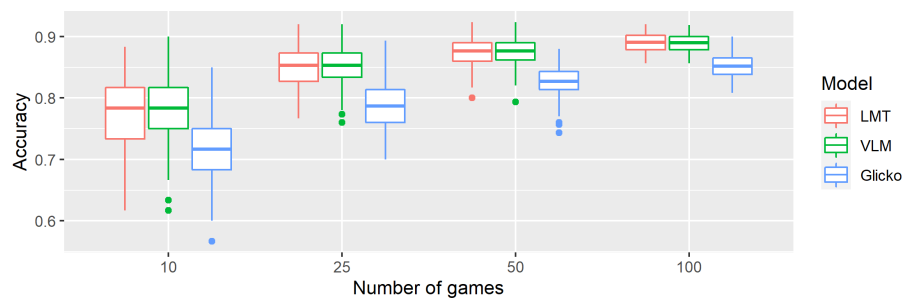


FIG 12. Predictive performance of LM-T, LM, and GLO models for head-to-head data